

The Doping Effect of Copper on the Catalytic Growth of Carbon Fibers from Methane over a Ni/Al₂O₃ Catalyst Prepared from Feitknecht Compound Precursor

Yongdan Li,¹ Jiuling Chen, Liu Chang, and Yongning Qin

Department of Catalysis Science and Technology and State Key Lab on C1 Chemical Technology, School of Chemical Engineering, Tianjin University, Tianjin 300072, China

Received August 20, 1997; revised December 29, 1997; accepted April 27, 1998

The doping effect of copper on the structure of a nickel-alumina catalyst, which was prepared from Feitknecht compound precursor with a hydrotalcite-like layered structure and on the catalytic growth of carbon fibers from methane have been investigated. An *in-situ* thermal balance was employed in the study of the carbon fiber growth process. It has been found that the addition of a small amount of copper into the nickel-alumina catalyst promotes the activity and that more than 36 wt% of CFs was produced when 2 mol% copper was added into a catalyst with a Ni/Al molar ratio of 3 : 1. Too much copper was found to decrease the activity of the catalyst toward solid carbon formation. The amount of carbon fibers produced on the catalyst, before its deactivation, decreases with the increase of the reaction temperature. When hydrogen instead of nitrogen was used as the dilution gas, the activity of the catalyst decreased and the reaction temperature had to be increased. The addition of copper lowers the effect of hydrogen. TEM micrographs showed that small particles are easier to activate than larger ones in the reaction. The possible effect of alloying between copper and nickel is discussed. © 1998 Academic Press

Key Words: catalytic growth of carbon fibers; nickel-copper-alumina catalyst; Feitknecht compound; alloying effect; methane.

1. INTRODUCTION

Carbon fibers (CFs) grown over metal particles such as Fe, Co, and Ni from the decomposition of hydrocarbons have been interesting materials in recent years (1–4). Several novel carbon structures such as fullerenes and nanotubes have been found in similar systems, and bringing excitement to many fields (5–9), due to their extraordinary physical and chemical properties. Efforts have been made to control the morphology and size of the nanotubes and to improve the efficiency of the production processes (2, 3, 10).

It has been proposed that the growth process was composed of several elementary steps. Hydrocarbons are dissociatively adsorbed on the surface of metal particles; then the adsorbed carbon atoms diffuse continuously through

the particle and precipitate at a particular crystal face to form CFs, and the deactivation of the metal occurs due to encapsulation by a graphite layer (3). A bulk-diffusion-controlled mechanism has been proposed (3, 11). Iron has a high activity at a temperature of around 1373 K (12–13), while nickel is active at lower temperature (14). A nickel catalyst prepared by coprecipitation, which can produce an interesting texture of CFs at low temperature, has been drawing attention (15–17). In this catalyst the active component is uniformly scattered and piled without order, so that CFs grow in random directions (15, 18–20) and tend to take the form of loops. As a result, the CFs produced in this way are woven into each other randomly to become lumps (15). It has been reported that the bulk crushing strength (BCS) of the CF lumps produced at 843 K on a nickel catalyst from methane is, when 0.5% fines formed, around 0.95 MPa, which is comparable to the BCS of commercially available support materials (15). The surface area of CFs thus formed can be as much as 300 m²/g, which can still be improved by a careful activation in carbon dioxide to around 700 m²/g (21). Further, it has been found that the CFs produced on the nickel catalyst have good adsorption properties to some organic molecules, such as benzene and toluene (22, 23), and inorganic molecules, such as CO, NO, NH₃ (24). It is expected that the CFs thus formed have excellent potentials both as catalyst support and as adsorbent.

A lot of knowledge has been accumulated from various studies on the principles that limit the formation of carbon fibers on various nickel catalysts, such as the steam reforming ones (11, 25–29). Pure nickel foil or powder has a low activity to generate CFs; however, when another component is added into it, its activity increases dramatically (17). When copper is incorporated into nickel by coprecipitation, a large amount of CF can be formed in a feed containing both ethylene and hydrogen (17). Avdeeva *et al.* (18) reported that when using a coprecipitated nickel-alumina or nickel-copper-alumina catalyst with high nickel content, around 250 g/gcat of CFs can be produced by

¹ Corresponding author. E-mail: ydli@tju.edu.cn.

decomposition of methane at 823 K, with a growth rate near 10 g/gcat.h.

In our recent work (20, 30), the growth of CFs from methane on a nickel-alumina catalyst prepared from a Feitknecht compound (FC) precursor has been discussed. With this catalyst a higher growth rate of CFs has been observed than that recently reported by Avdeeva *et al.* (18). FC was found as natural ionic clays with layered structure; it was also often called hydrotalcite-like compounds (31). These kinds of compounds have brucite-like layers containing octahedrally coordinated bivalent and trivalent cations, as well as interlayer anions and water. In its brucite-like layer, the cations have a uniform distribution (31). Due to the difficulty of solid phase diffusion of metal ions, this precursor results in a well-mixed oxide phase after calcination. Moreover, the well-mixed oxides form a paracrystalline metal phase during reduction (32) in which irreducible domains like $\text{Al}^{3+}\text{O}_x^{2-}$ exist and thus maximize the interaction of the components and, hence, the effect of dopants. Some work on the doping effect of copper on the nickel-alumina catalyst based on FC structure has been done in order to attain an intimate contact and mixing of the components. This paper reports the results and understanding on the effect of doping with copper for the formation of CFs from methane.

2. EXPERIMENTAL

2.1. Catalyst Samples

The precursors with the FC structure were obtained by coprecipitation from a mixed aqueous solution of nitrates by sodium carbonate. The precursors for pure nickel and copper oxides were prepared under the same condition. The precipitates were washed carefully to remove Na^+ and NO_3^- , dried in air at 393 K for 5 h and calcined at 723 K for 10 h. The powder thus obtained was pressed at 1.5 kbar into cylindrical tablets with a diameter of 8 mm and a length of 10 mm. The tablets were crushed and sieved into particles with a size distribution of 260–270 mesh. Table 1 lists the composition of the catalysts used in this work

2.2. Characterization

A D/MAX-2038 X-ray diffractometer with Fe $\text{K}\alpha$ was used to get the XRD profiles of the catalyst precursors and

the catalysts. The morphology of the CFs grown on the catalyst surface was studied with a PHILIPS 400 st transmission electron microscope (TEM).

TPR of the samples was carried out in a “U” shaped reactor with an internal diameter of 4 mm at a heating rate of 10 K/min and a total flow of 50 ml/min (STP) of 10 vol% of hydrogen in nitrogen. The size of the catalysts was between 40 and 60 meshes, determined by sieving method. The amount of catalyst used for each TPR experiment was 200 mg.

2.3. Reaction Conditions

The methane and nitrogen used in the experiments were nominally 99.999% pure. The hydrogen was 99.99% in purity. A catalytic oxygen removing purifier was incorporated before the inlet to the reaction unit. The experiments were carried out with a traditional thermal balance. An *in-situ* quartz reactor with a diameter of 20 mm and a length of 160 mm was located in a vertical furnace. The fine catalyst particles were placed in a quartz basket with a diameter of 12 mm and a height of 12 mm, which was positioned in the middle of the heated zone. The amount of catalyst in the oxidized state used for each experiment was about 3 mg. The reactor system was first purged with nitrogen. The reactor was then heated at a rate of 5 K/min to the reduction temperature 973 K in a gas flow, which contained 25 vol% of hydrogen and 75 vol% of nitrogen. The temperature was held about 30 min to allow the catalyst to be reduced, and then the temperature in the reactor was adjusted to the preset value in an atmosphere of pure nitrogen. The reaction was started on switching the gas flow to the diluted methane. The weight of the carbon fibers and the catalyst was measured continuously by the thermal balance. When the weight of the reactive samples did not change, the reaction was terminated. Methane was stopped first, and the nitrogen flow was allowed to continue until the temperature of the quartz reactor was lowered to ambient.

Several experiments were done at constant temperatures with a mixture of methane and nitrogen in a volume ratio of 1 : 2. Some other reactions were carried out with a constant heating rate of 5 K/min under a flow of methane and hydrogen in a volume ratio of 1 : 2. For all the reactions, the catalyst was reduced by the same procedure, and the total flow rate was 45 ml/min (STP). The reactions were performed at atmospheric pressure. An experiment was carried out at a constant temperature 773 K with a cofeed of methane and nitrogen, and was stopped after 5 min of reaction. The sample was used for TEM observation.

3. RESULTS

3.1. Structure of the Catalyst Precursors

Figure 1 gives the XRD profiles of the precipitated catalyst precursors before calcination. It shows that the first

TABLE 1

The Composition of the Catalyst Samples

Samples	Molecular ratio of $\text{M}^{2+}/\text{M}^{3+}$ in samples	
1	$\text{Ni}^{2+} : \text{Al}^{3+}$	75 : 25
2	$\text{Ni}^{2+} : \text{Al}^{3+} : \text{Cu}^{2+}$	75 : 23 : 2
3	$\text{Ni}^{2+} : \text{Al}^{3+} : \text{Cu}^{2+}$	75 : 10 : 15
4	Only Ni^{2+}	—
5	Only Cu^{2+}	—

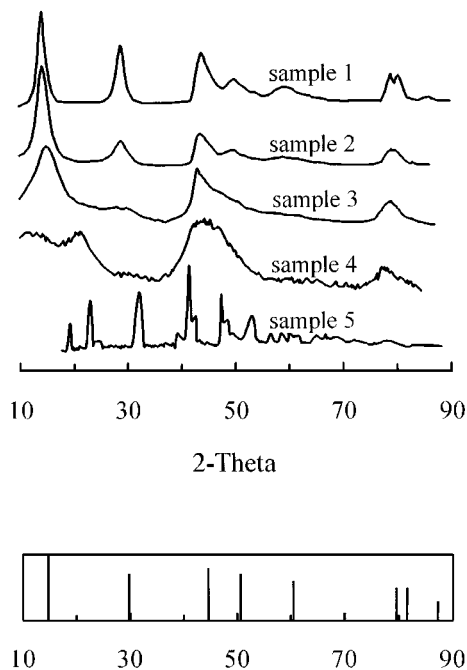


FIG. 1. The XRD patterns of the precipitated precursors. Lower part is the standard profile of FC phase, $\text{Ni}_6\text{Al}_2(\text{OH})_{16}\text{CO}_3 \cdot 4\text{H}_2\text{O}$, card number 15-87.

three samples containing aluminum have a typical FC structure, while in samples 4 and 5, those were precipitated under an exactly same condition, but without aluminum, only poorly crystallized metal hydroxide carbonates can be identified by XRD. Figure 1 shows also that the crystallinity of the samples with a FC structure reduces with an increasing molar ratio of $\text{M}^{2+}/\text{M}^{3+}$, i.e. when increasing the amount of copper.

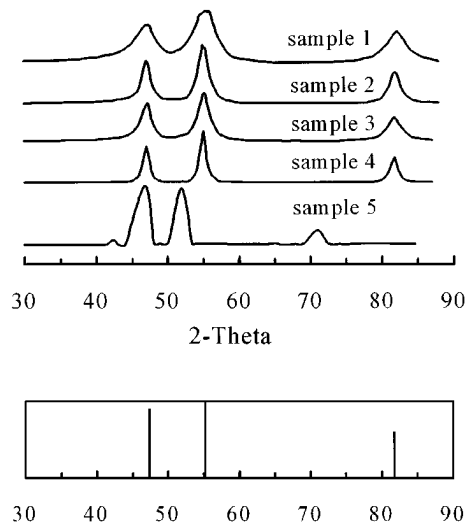


FIG. 2. The XRD patterns of the mixed oxides. The lower part is the standard profile of NiO, card number 4-835.

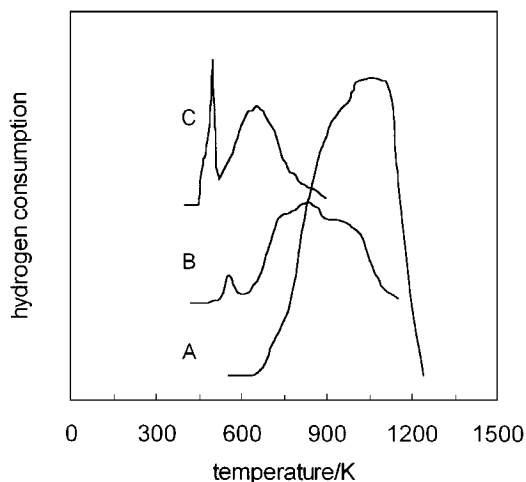


FIG. 3. The TPR curves of the mixed oxides: A, sample 1; B, sample 2; C, sample 3.

The XRD profiles of the corresponding mixed oxides after calcination are shown in Fig. 2. The profiles of samples 1, 2, and 3 show major peaks at nearly the same positions as NiO and have no peaks visible for Al_2O_3 or CuO. Samples 4 and 5 resulted in nearly perfectly crystallized NiO and CuO, respectively. These profiles indicate that well-crystallized FC results in wide diffraction peaks after calcination, which means more defects or distortions of the crystal lattice. Sample 3, which has 15 mol% of Cu^{2+} and was a poorly crystallized FC, resulted in a XRD profile very similar to that of pure NiO.

3.2. TPR Results of the Mixed Oxides

Figure 3 illustrates the TPR curves of the samples obtained from FC structured precursors. The figure shows that sample 1 has only one peak and began to be reduced at about 663 K. Its reduction rate reached a maximum in the range 1032–1093 K, and this process ended at near 1243 K. The curve of sample 2 shows two peaks, a small one in between 513 and 593 K, with its peak at around 555 K, the other one starting from 593 K and ending at near 1173 K, with its peak stretching from 748 to 886 K. Two peaks are also observed for sample 3, one from 455 to 528 K and the other one starting at 528 K and ending at 883 K, with their peaks at 503 and 668 K, respectively. Figure 4 presents the TPR curves of the two pure oxides, CuO and NiO, it can be seen that NiO was reduced between 573 and 773 K, with a maximum rate at 703 K; while CuO was reduced between 458 and 793 K, with a maximum rate at 673 K. The shapes of the two curves of CuO and NiO are rather similar.

3.3. CF Growth on the Catalysts

3.3.1. Methane and nitrogen as reactant. Figure 5 shows the weight gain process of the first three samples at a fixed temperature of 773 K. It can be seen that the first two

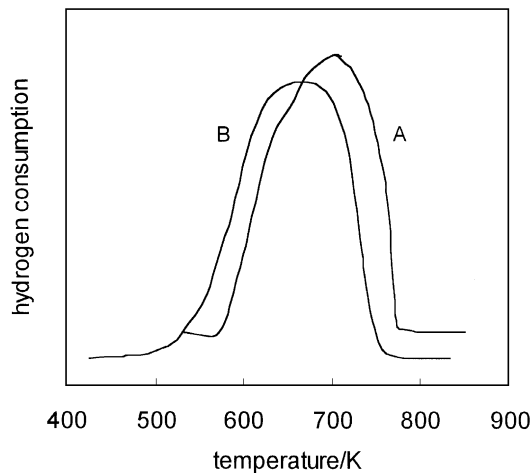


FIG. 4. The TPR curves of the pure oxides: A, sample 4; B, sample 5.

samples grow CFs at a comparable rate for a rather long time period. The growth rate of CFs on sample 3 is much lower than on the former two samples. Among the three samples, sample 2 retains its high activity for the longest time; however, they all deactivated after different reaction times. At the end of the reaction, the weight of CFs produced on samples 1, 2, and 3 reached values of 56, 76, and 17 times that of the original samples before reduction, respectively. These results indicate that a critical amount of copper is favorable to the CF formation.

To investigate the influence of the reaction temperature on activity and stability of the catalysts, experiments were performed at 873 K. The results are shown in Fig. 6. At the end of the reactions, or when the growth of CF stopped, the weight of CFs produced on samples 1, 2, and 3 reached values of 28, 41, and 13 times that of the original samples before reduction, respectively, showing a faster deactivation than in the 773 K reactions. The average growth rates

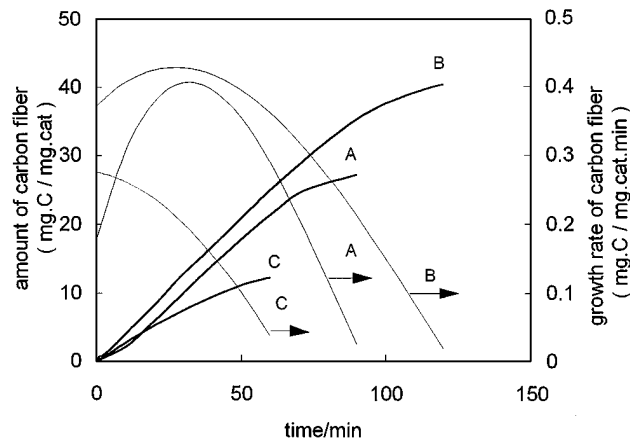


FIG. 6. Amount and growth rate of CF on different samples at 873 K: A, sample 1; B, sample 2; C, sample 3.

were, however, higher than for the individual samples at the reaction temperature of 773 K.

3.3.2. Methane and hydrogen as reactant. Due to the fact that all these samples showed no activity at 773 and 873 K when using a reactant of methane and hydrogen mixture, experiments were done with a constant heating rate. Figure 7 depicts the results. Over sample 1, carbon began to grow at 993 K and was deactivated at 1033 K. The final weight of carbon deposited was about twice that of the original sample before reduction. Over sample 2, carbon appeared at 973 K and the weight of CFs produced reached around 5 times that of the catalyst until the catalyst was deactivated at 1033 K. Under the same condition, CFs started to be formed at 923 K over sample 3 and went on growing up to 1113 K. The weight of CFs produced was 28 times that of the catalyst when the reaction was stopped. Higher temperatures were not explored due to the limit of the working range of the thermocouple used in our apparatus.

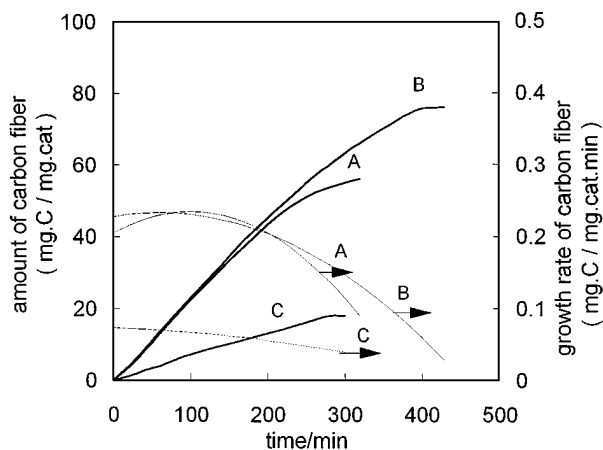


FIG. 5. Amount and growth rate of carbon fibers on different samples at 773 K: A, sample 1; B, sample 2; C, sample 3.

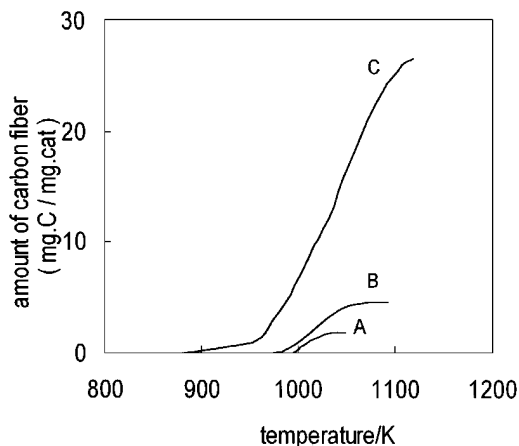


FIG. 7. The amount of CFs formed on different samples under a constant heating rate 5 K/min: A, sample 1; B, sample 2; C, sample 3.

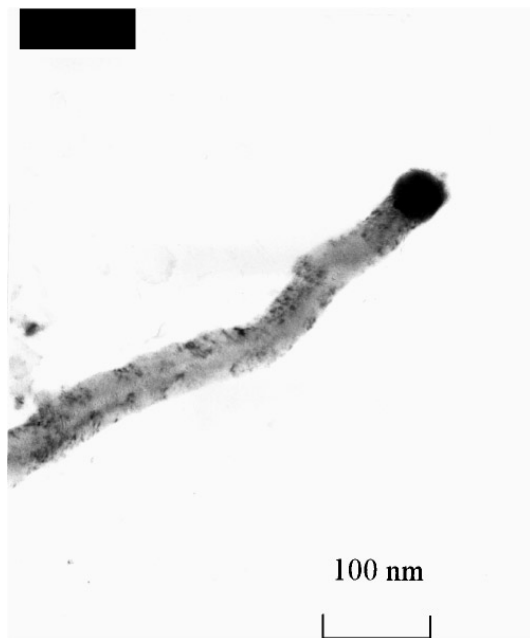


FIG. 8. A TEM micrograph showing the appearance of a CF produced at 773 K.

3.4. Characterization of the Produced CFs by TEM

The CFs grown were examined by TEM to determine their shapes. It was found that all the CFs are consisted of curved and hollowed tubes, each with a catalyst particle located at its tip, as shown in Fig. 8. The diameter of the CFs is governed by the size of the associated catalyst particle and typically in the range of 10 to 60 nm. In Fig. 9, photos A and B illustrate the CFs formed on sample 2 at 773 K in methane and nitrogen after the reaction was started for 5 min. At this point the weight of CFs formed was about 2.5 times that of the catalyst. Photo C and D show the CFs produced on sample 2 under the same conditions, but after the deactivation of the catalyst. A majority of the CFs in C and D are thicker than in A and B, indicating that smaller particles are activated earlier.

4. DISCUSSION

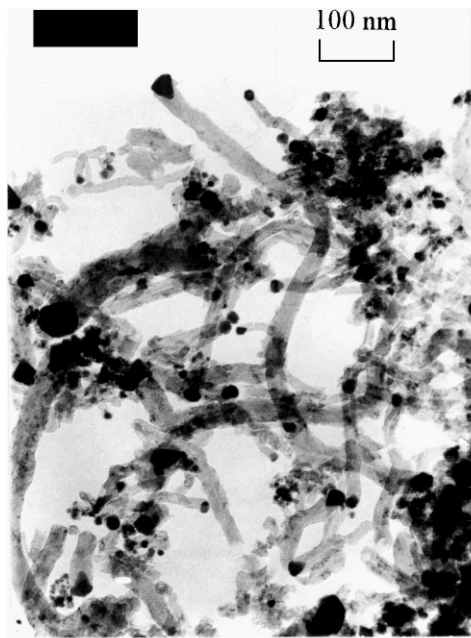
4.1. The Structure of the Catalyst and the Precursors

The doping of copper into the FC structured precursors by the coprecipitation process changes the crystallinity a little as presented in Fig. 1. This modification effect gets more important as the amount of the copper increases. This effect is interrelated with that of the reduced amount of aluminum. It seems likely from the XRD profiles that the precipitate of pure nickel has a structure or a profile similar to FC and that the precipitate of pure copper has a completely different structure. However, it is difficult to identify the exact structure of both the nickel and the copper precipitates due to their poor crystallinity. The XRD results

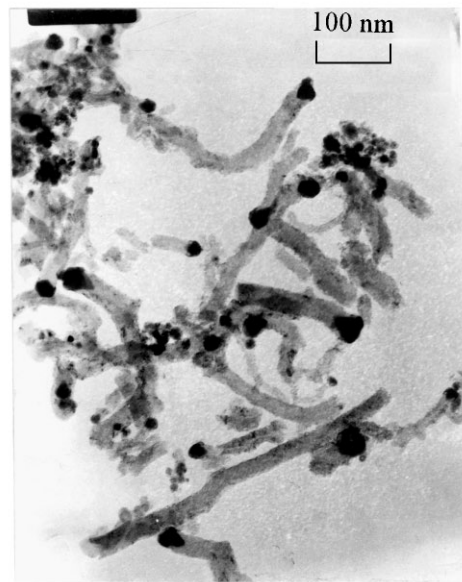
presented here are consistent with one of our recent proposals that the distorted FC structure allows a variation of the composition in a rather large range (20). Cavani *et al.* (31) did statistics of the possible ratio of M^{2+}/M^{3+} reported in the literature and proposed that the M^{2+}/M^{3+} in a range of 2–4 is critical for getting a pure FC phase; however, our experience with these FCs strongly support the idea that the ratio allowed in the structure is a dependent factor of preparation conditions.

The XRD profiles of the catalyst samples in the oxide state presented in Fig. 2 show that the phases often mentioned in the literature such as spinels, CuO, and Al_2O_3 are nonexistent in this case. The mixed oxides exist in a uniform NiO-like phase due to a strong interaction between the composing oxides. This phenomenon is consistent with the model proposed by Puxley *et al.* (32), which suggests that the mixed oxides obtained by calcination of nickel-aluminum FC are dispersed uniformly and adopt a metastable and distorted structure. This mixed oxide phase has the features of both NiO and $NiAl_2O_4$ (32). The introduction of copper does not appear to change this structure to any significant extent. Furthermore, the degree of crystallinity of the NiO-like phase after calcination improves as the proportion of divalent cations increases. It is interesting to note that copper oxide loses its structural features completely, even if the content of it is larger than aluminum, as in sample 3. From Fig. 2, the same conclusions as proposed in (20, 33) can be drawn that a well-crystallized FC results in a severely distorted NiO structure and that the increased amount of the divalent cations decreases the crystallinity of FC but increases the crystallinity of the mixed oxides obtained after a calcination process.

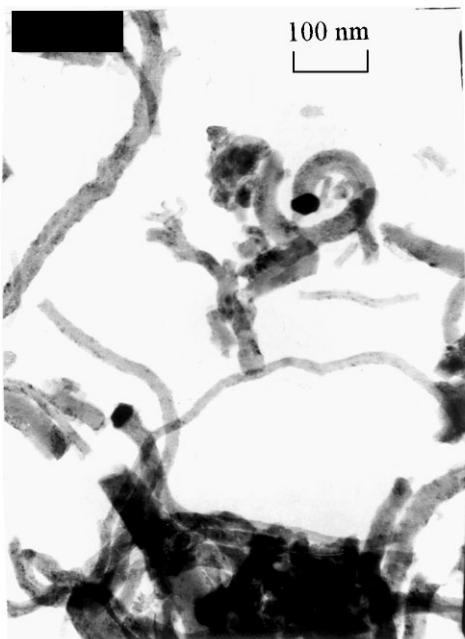
It is well established that nickel and copper tend to form alloys over a wide composition range (34). Incorporation of copper into the catalyst for CF growth was based on the facile formation of Ni/Cu alloy, the possibility of filling the d holes of nickel by an alloying effect, and the easy donation of electrons from copper in the alloy state (35–39). However, we find with TPR, depicted in Figs. 3 and 4, that the copper tends to reduce first from the uniformly mixed oxides and that the reduction of copper lowers the reduction temperature of nickel. This tailoring effect, caused by the addition of an easily reducible metal to an oxide which is more difficult to reduce, has been utilized in many metal catalysts. Although this effect and the existence of alloying effects need to be verified further, it is unreasonable to say that two metals form an alloy, if they are reduced with a large temperature difference from a mixed oxide state. Several points can be understood from the inspections of Figs. 3 and 4. The reduction profiles of pure nickel and copper only have a small difference in the way that the curve of nickel is “shifted” a little bit to a higher temperature range from the curve of copper. Formation of mixed oxides of nickel with aluminum from the FC precursor leads to



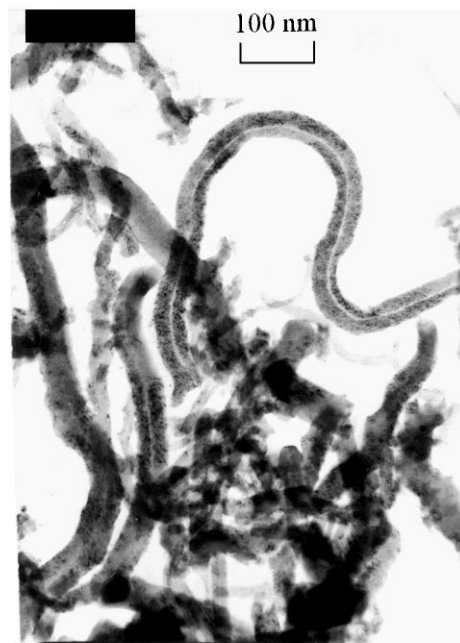
A



B



C



D

FIG. 9. TEM micrographs of the as-grown CFs: A and B, CFs on sample 2 after 5-min reaction at 773 K; C and D, CFs after the deactivation of sample 2 at 773 K.

a shift of about 300 K of the reduction profile of nickel to the higher temperature range. Incorporation of copper to the mixed oxides gives double peaked profiles. The first peak, with a lower temperature than that of the reduction of pure CuO, can be definitely attributed to the reduction of CuO. The second peak is the reduction of NiO. The reduced copper promotes the reduction of nickel from the mixed oxides and lowers its reduction temperature. This promotion effect gets stronger as the amount of copper introduced is increased. It is reasonable to assume that the composite catalyst after reduction has both the promoting effect of irreducible alumina, keeping the paracrystallinity (32) and the enhancing effect of hydrogen mobility of copper in a close vicinity. This reasoning does not exclude the possibility of a small proportion of copper staying in an alloy state with nickel, due to the well-mixed feature of the precursor.

4.2. Formation of CF on the Catalyst

It has been proposed that the size of the catalyst particles governs the diameter of CFs as a consequence thin CFs are favored by small particles (3, 40). It is reasonable to say that the metal particles, being lifted from the bulk of the catalyst by the growing of CFs, cannot possibly segregate to form bigger ones. The vapor-phase deposition of carbon can be excluded at 773 K. Therefore, the thick CFs are grown from the big particles. Inspection of the TEM pictures in Fig. 9 suggests that small catalyst particles are first activated and thin CFs are produced on them in the beginning stage of the reaction; afterwards, the bigger ones are activated. This is in accordance with the phenomenon observed by Avdeeva *et al.* (18). Because of the CFs for TEM observation are broken during the preparation of samples, the length of them cannot be measured. It should be noted that the TEM photos show that the CFs formed with the catalysts containing copper have a much smaller internal diameter than those grown on the catalysts without copper (20, 41). It seems likely that the thickness of the walls of the CFs are governed by the composition of the catalyst.

Inspections of Figs. 5 and 6 indicate that all the samples deactivated more quickly at 873 K than at 773 K. It can be calculated that, as the reaction temperature increased from 773 to 873 K, the amount of CFs produced before deactivation on sample 1 decreased by a factor of 48%, while on sample 2 and sample 3, they decreased 46 and 30%, respectively. These observations support that a higher reaction rate leads to faster deactivation, due to the encapsulation of the catalyst particles by an inert layer of carbon. It is interesting to note also that the addition of copper lowers the effect of the reaction temperature for CF formation.

4.3. Effect of Copper on the Activity

From the results presented in Figs. 5 and 6, it can be found that a suitable amount of copper can promote the

activity in the CF growth process, but too much copper decreases the activity. We have reported that a small amount of alumina can promote the activity and lower the reaction temperature of nickel in the CF growth reaction from methane and we attributed this effect to a strong interaction between nickel and alumina inherited from the FC precursor (20). Here, the copper is also introduced with a same precursor; thus, both the effect of alumina and copper can be expected to exist in the reaction. Copper has been used widely as the active component of hydrogenation catalysts (31, 33); it enhances the hydrogen mobility. It has been also proposed that copper has a high affinity with the graphite structure, thereby inhibiting the formation of a graphite layer on nickel surface [19] and, thus, showing copper to be a good third component when in an appropriate amount.

4.4. The Role of Hydrogen in the Reaction

With hydrogen replacing nitrogen in the feed, a strong retarding effect has been observed; this is in accordance with our previous observations with a nickel-alumina catalyst (20). When hydrogen and methane are used as the reactant, CFs start to grow on sample 1 at a temperature as high as 993 K, and only a very small amount of CF is formed until the reaction is stopped due to deactivation. The substitution of nickel with copper by 2 mol% in sample 2 has a small effect by slightly increasing the CF formation and lowering the starting temperature of the reaction. However, sample 3, which has a rather large content of copper, initiates the reaction at a lower temperature and produces a comparatively large amount of CF at a higher temperature range. These results are illustrated in Fig. 7. The activation temperatures of the catalysts are much higher under these reaction conditions than that observed with a methane and nitrogen mixture. From a practical standpoint there may be some benefits if the reaction can be performed at round 1073 K and without the inert gas nitrogen, because the conversion of this reaction is limited by thermodynamics, and it should be possible to reach a methane conversion of about 90% at a temperature higher than 1073 K (42). In this case, hydrogen is formed with a high purity and can be used directly as the feed stocks in many hydrogenation reactions.

The results presented here are in accordance with the literature, that the presence of hydrogen can maintain a catalytically active copper-nickel alloy at a high temperature (39). This effect may come from the enhanced reverse reaction of the methane decomposition and in this way prevent the surface from being encapsulated by the accumulation of carbon as a blocking film.

5. CONCLUSIONS

The introduction of copper into a nickel-aluminum FC structured phase, in which all the cations are uniformly distributed during the coprecipitation process, can be

performed under a precisely controlled condition. An introduction of copper distorts the FC crystal lattice. After calcination, the FC structured precursors become a distorted nickel oxide-like phase. Well-crystallized FC gives a seriously distorted nickel phase. No copper oxide-like and alumina-like phases exist in the calcined samples. This suggests a uniformly mixed oxide phase and a strong interaction of the components formed. The nickel-aluminum mixed oxide without copper reduces at a temperature of 300 K higher than that of pure nickel oxide; in contrast, the mixed oxides with copper exhibit double peaks in TPR, where the lower temperature peak is lower than that of the reduction of pure copper oxide and the other peak is higher than that of pure nickel oxide. The formation of an alloy in the reduction is thus doubtful; however, the promotion effect from adjacent copper to nickel is possible.

The addition of 2 mol% copper into a Ni-alumina catalyst with a Ni/Al molar ratio 3:1 promotes the activity of CF growth. At 773 K, the weight of CFs produced on this catalyst reached a maximum value of 76 times that of the original sample before reduction, which is 36% more than the same catalyst without copper. Too much copper decreases both the activity and the amount of CFs formed before deactivation. It has also been observed that higher temperatures than 773 K leads to a higher reaction rate but a shorter life of the catalyst.

Hydrogen inhibits the formation of CFs on the nickel catalysts in a way that it increases the activation temperature and lowers the reaction rate and the amount of CF formed before deactivation. The incorporation of copper into the catalyst reduces the effect of hydrogen. An interesting result was obtained with a catalyst having a large ratio of copper to nickel that it produces CFs with a considerable high rate in a temperature range around 1073 K and with hydrogen feeding. This may be favored for commercial application since a pure hydrogen stream can be produced which is useful in many processes.

ACKNOWLEDGMENT

This work was supported in part by NSF of China.

REFERENCE

1. Tibbets, G. G., Endo, M., and Beetz, C. P., Jr., *Sampe J. Sept/Oct.*, 30 (1986).
2. Endo, M., *Chemtech Sept.*, 568 (1988).
3. Baker, R. T. K., *Carbon* **27**, 315 (1989).
4. Rodriguez, N. M., *J. Mater. Res.* **8**, 3233 (1993).
5. Iijma, S., *Nature* **354**, 56 (1991).
6. Ebbesen, T. W., and Ajayan, P. M., *Nature* **358**, 220 (1992).
7. Weaver, J. H., *Science* **265**, 611 (1994).
8. Wang, X. K., Lin, X. W., Dravid, V. P., Ketterson, J. B., and Chang, P. H., *Appl. Phys. Lett.* **62**, 1881 (1993).
9. Nagy, J. B., Ivanov, V., and Zhang, X. B., *Science* **265**, 635 (1994).
10. Tibbets, G. G., *Carbon* **27**, 745 (1989).
11. Rostrup-Nielsen, J. R., and Trimm, D. L., *J. Catal.* **48**, 155 (1977).
12. Masuda, T., Mukai, S. R., and Hashimoto, K., *Carbon* **31**, 783 (1993).
13. Tibbets, G. G., *Appl. Phys. Lett.* **42**, 666 (1983).
14. Jablonski, G. A., *Carbon* **19**, 99 (1992).
15. Hoogenraad, G. S., thesis, Universiteit Utrecht, The Netherlands, 1995.
16. Shaikhutdinov, Sh. K., Avdeeva, L. B., Goncharova, O. V., Kochubey, D. I., Novgorodov, B. N., and Plyasova, L. M., *Appl. Catal. A* **126**, 125 (1995).
17. Kim, M. S., Rodriguez, N. M., and Baker, R. T. K., *J. Catal.* **131**, 60 (1991).
18. Avdeeva, L. B., Goncharova, O. V., Kochubey, D. I., Zaikovskii, V. I., Plyasova, L. M., Novgorodov, B. N., and Shaikhutdinov, Sh. K., *Appl. Catal. A* **141**, 117 (1996).
19. Kim, M. S., Rodriguez, N. M., and Baker, R. T. K., *J. Catal.* **134**, 253 (1992).
20. Li, Y. D., Chen, J. L., and Chang, L., *Appl. Catal. A General* **163**, 45 (1997).
21. Rodriguez, N. M., Kim, M. S., and Baker, R. T. K., *J. Phys. Chem.* **98**, 13108 (1994).
22. Fenelonov, V. B., Avdeeva, L. B., and Zheivot, V. I., *Kinet. Katal.* **34**, 542 (1993).
23. Fenelonov, V. B., Avdeeva, L. B., Goncharova, O. V., Okkel, L. G., Simonov, P. A., Derevyankin, A. Y., and Likhoholobov, V. A., *Stud. Surf. Sci. Catal.* **91**, 825 (1995).
24. Bagrii, E. I., Tretyakov, I. F., Trusova, E. A., Popov, V. T., and Slovetsk, D. I., *Neftekhemia* **31**, 236 (1991).
25. Trimm, D. L., *Catal. Rev. Sci. Eng.* **16**(2), 155 (1977).
26. Bartholomew, C. H., *Catal. Rev. Sci. Eng.* **24**(1), 155 (1982).
27. Zhuang, Q., Qin, Y. N., and Chang, L., *Appl. Catal.* **70**, 1 (1991).
28. Wu, X. Y., Zhang, J. Y., and Chang, L., *Stud. Surf. Sci. Catal.* **34**, 208 (1987).
29. Dong, G. X., and Chang, L., *Huagong Xuebao* **4**, 459 (1985). [Chinese]
30. Li, Y. D., Chen, J. L., and Chang, L., in "Advances in Catalysis Research" (H. B. Zhang, J. X. Cai, D. W. Liao, and H. L. Wan, Eds.), p. 433. Xiaman Univ. Press, Xiamen, 1996. [Chinese]
31. Cavani, F., Trifiro, F., and Vaccari, A., *Catal. Today* **11**, 173 (1991).
32. Puxley, D. C., Kitchener, I. J., Komodromos, C., and Purkgn, N. D., *Stud. Surf. Sci. Catal.* **16**, 227 (1983).
33. Zhao, J. S., Li, Y. D., Ma, F. S., Kang, H. M., and Zhu, C. L., *Ranliao Huaxue Xuebao (Fuel Chemistry and Technology)* **14**(3), 201 (1986). [Chinese]
34. Khulbe, K. C., and Mann, R. S., *Catal. Rev. Sci. Eng.* **24**, 311 (1982).
35. Alstrup, I., and Tavares, M. T., *J. Catal.* **139**, 513 (1993).
36. Nishiyama, Y., and Tamai, Y., *J. Catal.* **45**, 1 (1976).
37. Alstrup, I., *J. Catal.* **109**, 241 (1988).
38. Nishiyama, Y., and Tamai, Y., *J. Catal.* **33**, 98 (1974).
39. Rodriguez, N. M., Kim, M. S., and Baker, R. T. K., *J. Catal.* **140**, 16 (1993).
40. Krishnankutty, N., Rodriguez, N. M., and Baker, R. T. K., *J. Catal.* **158**, 217 (1996).
41. Cui, S., Li, Y. D., and Chang, L., *Chinese Sci. Bull.* **41**, 2011 (1996). [Chinese]
42. Zhao, J. B., Li, Y. D., and Chang, L., *Tianranqi Huagong* **22**(4), 48 (1997). [Chinese]